Langmuir
Article
pubs.acs.org/Langmuir

A Versatile Molecular Layer-by-Layer Thin Film Fabrication Technique Utilizing Copper(I)-Catalyzed Azide−Alkyne Cycloaddition

Peter K. B. Palomaki and Peter H. Dinolfo*

Department of Chemistry and Chemical Biology and The Baruch 60' Center for Biochemical Solar Energy Research, Rensselaer Polytechnic Institute, 110 8th Street, Troy, New York 12180

Received January 21, 2010. Revised Manuscript Received March 9, 2010

We have developed a rapid and versatile layer-by-layer (LbL) thin film fabrication method using copper(I)-catalyzed azide−alkyne cycloaddition (CuAAC) or "click" chemistry in the construction of molecular multilayer assemblies. Multilayers containing synthetic porphyrins, perylene diimides, and mixtures of the two have been constructed in order to highlight the versatility of this method. Characterization of thin films using UV−vis absorption, water contact angle, and electrochemical techniques indicate that multilayer growth is consistent over tens of layers. Preliminary X-ray reflectivity measurements yield an average bilayer thickness of 2.47 nm for multilayers of **1** and **3** grown on glass. Polarized absorption measurements suggest that the dense thin films exhibit moderate ordering in their molecular structure with partial alignment with respect to the surface normal.

Introduction

The layer-by-layer (LbL) fabrication of thin film materials has become an active area of research in recent years because of its ability to generate multicomponent thin films quickly and at relatively low cost. The ability to control accurately the growth and ordering of thin films at the molecular level has significant implications in the development of materials for, inter alia, nonlinear optics, photovoltaics, memory devices, sensors, and molecular electronics.[1−3] The LbL fabrication process is a bottom-up approach to surface functionalization that permits the modification of a substrate by adding alternating components in a binary reaction sequence such that molecules in solution react with the substrate-bound material to give multilayer thin films. LbL assembly methods can provide molecular level control of structure in one dimension from simple solution deposition processes when self-limiting reactions are employed. These methods permit the rapid and straightforward modification of substrate surfaces to regulate their physical, electronic, photophysical, and chemical properties.

LbL fabrication of molecular-based multilayer films, often referred to as molecular layer deposition (MLD), requires the use of self-limiting coupling reactions that result in the deposition of a single monolayer at each step. Different modes of molecular interaction have been employed in LbL techniques to create well ordered molecular multilayer assemblies. These include zirconium phosphate linkages,[4−8] palladium−pyridine coordination,[9−11] siloxane polymerization,[12−17] and various other organic reactions.[1,18−23]

What could be useful to the field of molecular LbL fabrication is an efficient and rapid method to couple layers together at ambient conditions with broad flexibility in the choice of building blocks. To this end, we have developed a versatile LbL thin film fabrication technique utilizing copper(I)-catalyzed azide−alkyne cycloaddition (CuAAC) or "click" chemistry to build molecular multilayers. Discovered by Sharpless[24] and Meldal,[25] CuAAC has become popular as a high-yielding coupling reaction between terminal azides and acetylenes to form 1,4-triazoles selectively.[26,27] The CuAAC reaction has several advantages, including an inexpensive coupling catalyst, easily incorporated and relatively inert functional groups, and quick and quantitative reactions at room temperature in a variety of solvents. While CuAAC has

*Corresponding author. E-mail: dinolp@rpi.edu.

(1) George, S. M.; Yoon, B.; Dameron, A. A. *Acc. Chem. Res.* **2009**, *42*, 498–508.
(2) Xi, Z.; Jiacong, S. *Adv. Mater.* **1999**, *11*, 1139–1143.
(3) Ariga, K.; Hill, J. P.; Ji, Q. *Phys. Chem. Chem. Phys.* **2007**, 2319–2340.
(4) Yang, H. C.; Aoki, K.; Hong, H. G.; Sackett, D. D.; Arendt, M. F.; Yau, S. L.; Bell, C. M.; Mallouk, T. E. *J. Am. Chem. Soc.* **2002**, *115*, 11855–11862.
(5) Lee, H.; Kepley, L. J.; Hong, H. G.; Akhter, S.; Mallouk, T. E. *J. Phys. Chem.* **2002**, *92*, 2597–2601.
(6) Neff, G. A.; Helfrich, M. R.; Clifton, M. C.; Page, C. J. *Chem. Mater.* **2000**, *12*, 2363–2371.
(7) Zeppenfeld, A. C.; Fiddler, S. L.; Ham, W. K.; Klopfenstein, B. J.; Page, C. J. *J. Am. Chem. Soc.* **1994**, *116*, 9158–9165.
(8) Katz, H. E.; Scheller, G.; Putvinski, T. M.; Schilling, M. L.; Wilson, W. L.; Chidsey, C. E. D. *Science* **1991**, *254*, 1485–1487.
(9) Altman, M.; Shukla, A. D.; Zubkov, T.; Evmenenko, G.; Dutta, P.; van der Boom, M. E. *J. Am. Chem. Soc.* **2006**, *128*, 7374–7382.
(10) Altman, M.; Zenkina, O.; Evmenenko, G.; Dutta, P.; van der Boom, M. E. *J. Am. Chem. Soc.* **2008**, *130*, 5040–5041.
(11) Motiei, L.; Altman, M.; Gupta, T.; Lupo, F.; Gulino, A.; Evmenenko, G.; Dutta, P.; van der Boom, M. E. *J. Am. Chem. Soc.* **2008**, *130*, 8913–8915.
(12) van der Boom, M. E.; Richter, A. G.; Malinsky, J. E.; Lee, P. A.; Armstrong, N. R.; Dutta, P.; Marks, T. J. *Chem. Mater.* **2000**, *13*, 15–17.
(13) Netzer, L.; Sagiv, J. *J. Am. Chem. Soc.* **1983**, *105*, 674–676.
(14) Li, D.; Ratner, M. A.; Marks, T. J.; Zhang, C.; Yang, J.; Wong, G. K. *J. Am. Chem. Soc.* **1990**, *112*, 7389–7390.
(15) Facchetti, A.; Abbotto, A.; Beverina, L.; van der Boom, M. E.; Dutta, P.; Evmenenko, G.; Pagani, G. A.; Marks, T. J. *Chem. Mater.* **2003**, *15*, 1064–1072.
(16) Zhu, P.; van der Boom, M. E.; Kang, H.; Evmenenko, G.; Dutta, P.; Marks, T. J. *Chem. Mater.* **2002**, *14*, 4982–4989.
(17) van der Boom, M. E.; Zhu, P.; Evmenenko, G.; Malinsky, J. E.; Lin, W.; Dutta, P.; Marks, T. J. *Langmuir* **2002**, *18*, 3704–3707.
(18) Kohli, P.; Blanchard, G. J. *Langmuir* **2000**, *16*, 4655–4661.
(19) Li, Y.-h.; Wang, D.; Buriak, J. M. *Langmuir* **2010**, *26*, 1232−1238.
(20) Schmidt, I.; Jiao, J.; Thamyongkit, P.; Sharada, D. S.; Bocian, D. F.; Lindsey, J. S. *J. Org. Chem.* **2006**, *71*, 3033–3050.
(21) Jiao, J.; Anariba, F.; Tiznado, H.; Schmidt, I.; Lindsey, J. S.; Zaera, F.; Bocian, D. F. *J. Am. Chem. Soc.* **2006**, *128*, 6965–6974.
(22) Li, D.; Swanson, B. I.; Robinson, J. M.; Hoffbauer, M. A. *J. Am. Chem. Soc.* **1993**, *115*, 6975–6980.
(23) Li, D.; Buscher, C. T.; Swanson, B. I. *Chem. Mater.* **1994**, *6*, 803–810.
(24) Rostovtsev, V. V.; Green, L. G.; Fokin, V. V.; Sharpless, K. B. *Angew. Chem., Int. Ed.* **2002**, *41*, 2596–2599.
(25) Tornoe, C. W.; Christensen, C.; Meldal, M. *J. Org. Chem.* **2002**, *67*, 3057–3064.
(26) Meldal, M.; TornÃe, C. W. *Chem. Rev.* **2008**, *108*, 2952–3015.
(27) Sumerlin, B. S.; Vogt, A. P. *Macromolecules* **2009**, *43*, 1–13.

Scheme 1. CuAAC-Based LbL Assembly Scheme

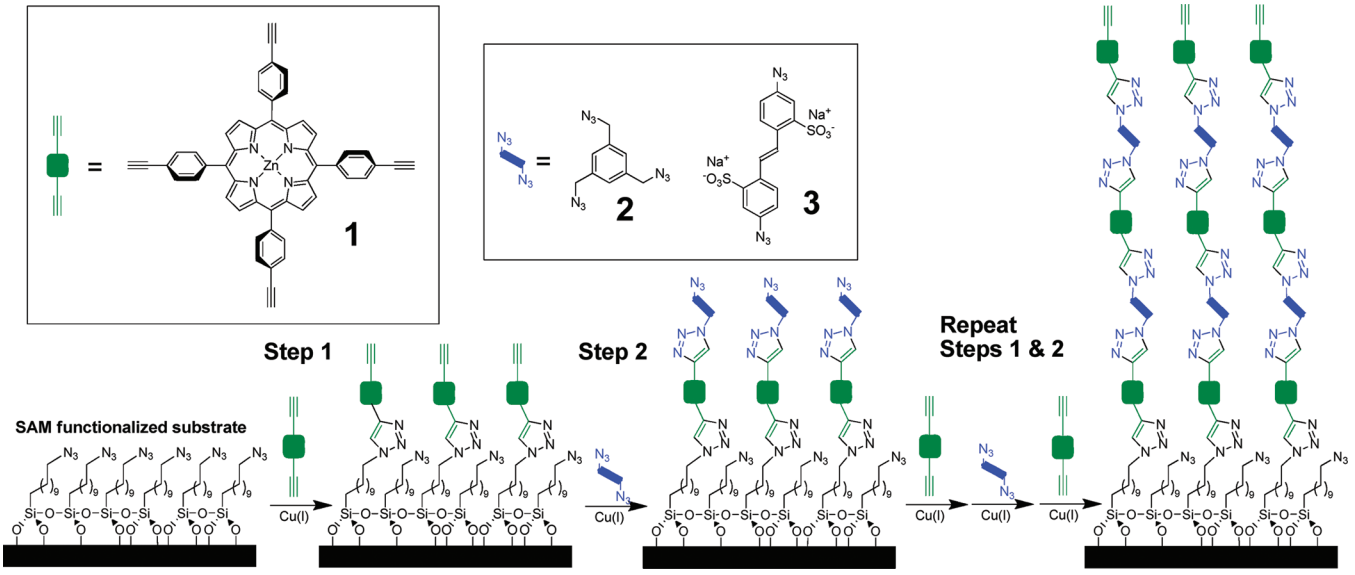

been used to build triazole-linked polymer multilayers,[28,29] it has not, to our knowledge, been used to assemble molecular multilayers. We demonstrate herein that this flexible coupling method enables the rapid growth of ordered multilayer films on oxide surfaces modified with an azide-terminated self-assembled monolayer (SAM) using a variety of molecular components.

CuAAC reactivity was first applied to surface modification through the covalent attachment of a wide variety of ethynyl terminated molecular species to Au(111) electrode surfaces coated with an azide-terminated SAM.[30−34] This technique provides a flexible procedure to tune the density of surface azide groups and thus the coverage of surface-tethered molecules following the CuAAC reaction. In those reports, CuAAC reactions of azide-modified substrates with ethynyl-functionalized molecules occurred on the time scale of minutes when the Cu(I) catalyst is accompanied by an amine stabilizing ligand, tris-(benzyltriazolylmethyl)amine (TBTA).[31,35] Subsequent studies have extended this surface modification technique to include oxide surfaces through the use of azido-alkylsiloxane SAMs.[34,36−38]

Following these reports, we surmised that CuAAC surface reactions could provide a convenient and flexible method for the generation of multilayer thin film materials in a LbL fashion. Scheme 1 outlines the process of building multilayers using CuAAC reactivity. First, an oxide surface (indium tin oxide or silica glass) is modified with an azide terminated alkylsiloxane SAM. Next, a multiacetylene functionalized molecule (such as **1**) is reacted with the azide modified substrate in the presence of a Cu(I) catalyst (step 1). This self-limiting reaction will create a monolayer of **1** covalently attached to the SAM modified substrate, yielding a surface which is now terminated with acetylene moieties. To regenerate an azide terminated surface, a molecule containing multiple azide groups (such as **2** or **3**), herein referred to as a linker, is reacted with the acetylene-terminated surface under similar CuAAC conditions (step 2). This two-step process yields a single molecular bilayer covalently attached to the surface via 1,4-triazoles and can be repeated indefinitely until the desired number of multilayers is achieved. Herein, we describe the initial results in the development of such an LbL assembly method. We believe that this technique has the potential to provide a rapid and highly flexible method for the formation of complex multilayer structures from simple molecular components and solution-based deposition techniques.

Experimental Section

General Methods. NMR spectra were obtained on a Varian 500 MHz spectrometer and the chemical shifts were referenced to the standard solvent shift. LR and HR MALDI-TOF MS were obtained on a Bruker Ultraflex III. LR and HR ESI MS were obtained on a Thermo Electron Finnigan TSQ Quantum Ultra. FTIR were obtained on a Thermo Nicolet 4700.

Materials. Solvents, ACS reagent grade or better, were purchased from Sigma Aldrich or Fisher Scientific and used as received. Anhydrous tetrahydrofuran (THF) and dicholoromethane (DCM) were purified by recirculating the nitrogen-purged solvent through a solid-state column purification system[39] (Vacuum Atmospheres Company, Hawthorne, CA) prior to use. Dry toluene was purged with nitrogen and stored over molecular sieves before use. 4-Iodoanaline (Aldrich), sodium ascorbate (Aldrich), 2,5-di-*tert*-butylhydroquinone (Aldrich), and 4,4′-diazido-2,2′-stilbenedisulfonic acid disodium salt tetrahydrate (**3**) (Fluka) were used as received. Tetrabutylammonium hexafluorophosphate (TBAP, Acros) was recrystallized twice from hot ethanol before use in electrochemical experiments. 11-Azidoundecyltrimethoxysilane,[40] Zn(II) 5,10,15,20-tetra(4-ethynylphenyl)porphyrin (**1**),[41] Zn(II) 5-(4-ethynylphenyl)-10,15,20-triphenyl

(28) Such, G. K.; Quinn, J. F.; Quinn, A.; Tjipto, E.; Caruso, F. *J. Am. Chem. Soc.* **2006**, *128*, 9318–9319.
(29) Bergbreiter, D. E.; Chance, B. S. *Macromolecules* **2007**, *40*, 5337–5343.
(30) Collman, J. P.; Devaraj, N. K.; Chidsey, C. E. D. *Langmuir* **2004**, *20*, 1051–1053.
(31) Collman, J. P.; Devaraj, N. K.; Eberspacher, T. P. A.; Chidsey, C. E. D. *Langmuir* **2006**, *22*, 2457–2464.
(32) Devaraj, N. K.; Decreau, R. A.; Ebina, W.; Collman, J. P.; Chidsey, C. E. D. *J. Phys. Chem. B* **2006**, *110*, 15955–15962.
(33) Devaraj, N. K.; Dinolfo, P. H.; Chidsey, C. E. D.; Collman, J. P. *J. Am. Chem. Soc.* **2006**, *128*, 1794–1795.
(34) Devaraj, N. K.; Miller, G. P.; Ebina, W.; Kakaradov, B.; Collman, J. P.; Kool, E. T.; Chidsey, C. E. D. *J. Am. Chem. Soc.* **2005**, *127*, 8600–8601.
(35) Chan, T. R.; Hilgraf, R.; Sharpless, K. B.; Fokin, V. V. *Org. Lett.* **2004**, *6*, 2853–2855.
(36) Prakash, S.; Long, T. M.; Selby, J. C.; Moore, J. S.; Shannon, M. A. *Anal. Chem.* **2006**, *79*, 1661–1667.
(37) Lummerstorfer, T.; Hoffmann, H. *J. Phys. Chem. B* **2004**, *108*, 3963–3966.
(38) Ku, S.-Y.; Wong, K.-T.; Bard, A. J. *J. Am. Chem. Soc.* **2008**, *130*, 2392–2393.
(39) Pangborn, A. B.; Giardello, M. A.; Grubbs, R. H.; Rosen, R. K.; Timmers, F. J. *Organometallics* **1996**, *15*, 1518–1520.
(40) Fu, Y.-S.; Yu, S. J. *Angew. Chem., Int. Ed.* **2001**, *40*, 437–440.
(41) Onitsuka, K.; Kitajima, H.; Fujimoto, M.; Iuchi, A.; Takei, F.; Takahashi, S. *Chem. Commun.* **2002**, 2576–2577.

porphyrin (**4**),[42] tris-(benzyltriazolylmethyl)amine (TBTA),[35] and 1,3,5-tris(azidomethyl)benzene (**2**)[43] were synthesized according to literature methods. Glass microscope slides were purchased from Erie Scientific (precleaned) and ITO-coated glass slides were purchased from Delta Technologies (polished float glass, ITO coated one surface, $R_s = 4-8\ \Omega$).

Electronic Absorption Spectroscopy. Electronic absorption spectra were taken on a Perkin-Elmer Lamda 950 spectrometer with slides held against the wall of a quartz cuvette filled with DI water. A background spectrum of the SAM functionalized slide was subtracted from each spectrum. Polarized absorbance spectra were taken with the slide positioned at a 45° angle with respect to the incident light beam, and a background spectrum was subtracted for each angle at which a sample spectrum was taken. The incident light was polarized with a Glan-Taylor prism.

Contact Angle. Water contact angle measurements were made on a Rame-Hart model 100 goniometer with 2 μL drops of DI water. Reported values are an average of no less than four data points. Slides were washed with ethanol and dried in a stream of air prior to measurement.

Electrochemistry. Electrochemical measurements were performed using a CH Instruments 440A potentiostat in a three-electrode configuration. The working area of the ITO functionalized electrode was defined by the cylindrically bored area of a Teflon cone pressed on the sample surface and filled with electrolyte.[44] Multilayer thin film electrochemical experiments were performed in dry DCM with 0.1 M TBAP as the electrolyte with a Ag/Ag^+ pseudoreference electrode and a platinum wire counter electrode. Blocking layer experiments were carried out in degassed DI water with 0.1 M potassium chloride as the electrolyte, a Ag/AgCl (satd. NaCl) reference electrode, and a platinum wire counter electrode.

Specular X-ray Reflectivity. X-ray reflectivity (XRR) experiments were performed with a Bruker D8 Discover using a 2-circle $\theta/2\theta$ goniometer, a centric Eulerian cradle, and a sealed tube copper X-ray source (Cu Kα $\lambda = 1.54$ Å) operated at 40 kV. The resulting XRR data are normalized to the energy of the X-ray source where the wave vector transfer (q) is directly related to the incident angle, $q = 4\pi \sin(\theta)/(\lambda)$. Simulated XRR curves were generated using the Bruker Leptos software suite with a model consisting of two sample layers on top of a SiO_2 substrate. The first layer, representing the alkylsiloxane SAM, was fixed at 1.5 nm (experimental value found by XRR) and a density of 0.85 g/cm^3, which are reasonable values for alkylsiloxane monolayers.[45] The second layer represented the porphyrin multilayer film. Variables for thickness, roughness, and density were constrained to reasonable values during the fitting process which was performed on the reflectivity curve from approximately $2\theta = 0.4°$ (just below the critical angle) to a region where the fringe patterns could no longer be discerned from the noise. For the final reported fit curves, the following parameters were fit: SiO_2 roughness, SAM roughness, and multilayer thickness, roughness, and density.

Perylene Diimide Synthesis. 1,6- and 1,7-di(4-*tert*-butylphenoxy)-3,4:9,10-perylenetetracarboxylic dianhydride was synthesized in a manner similar to published procedures.[46−48] A mixture of 1,6- and 1,7- isomers was carried throughout all reactions and was used in multilayer fabrication without separation of isomers.

Scheme 2. Synthesis of a Perylene Diimide Featuring *trans* Ethynyl Functionalities

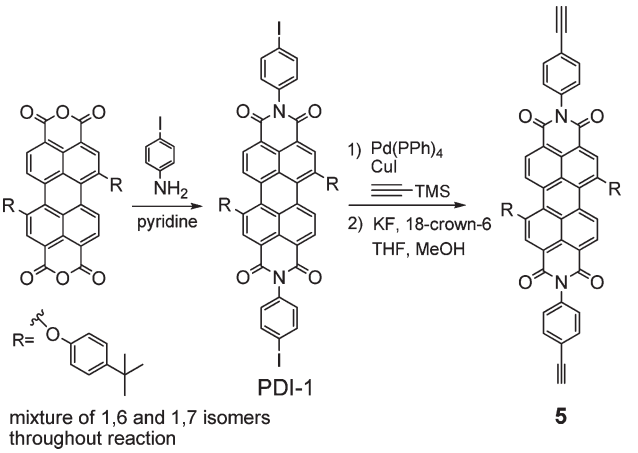

N,N′-Di(4-iodobenzene)-1,6-di(4-tert-butylphenoxy)-3,4:9,10-perylenebis(dicarboximide) and N,N′-Di(4-iodobenzene)-1,7-di(4-tert-butylphenoxy)-3,4:9,10-perylenebis(dicarboximide) (***PDI-1***). 1,6- and 1,7-di(4-*tert*-butylphenoxy)-3,4:9,10-perylenetetracarboxylic dianhydride (0.076 g, 0.106 mmol) and 4-iodoaniline (0.136 g, 0.621 mmol) were added to a round-bottom flask with pyridine (10 mL) and degassed with N_2. The purple solution was heated to reflux under a N_2 atmosphere for 6 days. Zinc acetate (0.040 g, 0.22 mmol) was added to the reaction during the seccond day. After cooling to room temperature, the red mixture was added to HCl (aq) (15 vol %, 15 mL) and a red/maroon precipitate formed. The precipitate was filtered and washed with water (3 × 15 mL) to yield a red/maroon solid. The crude product was chromatographed on silica and the desired products eluted first using chloroform (0.081 g, 70%, mixture of 1,7- and 1,6-isomers). ^{1}H NMR ($CDCl_3$): 9.64 and 9.58 d (4H, $J = 8.5$ Hz, pery-H_6 and pery-H_{12} 1,7 isomer; pery- H_7 and pery-H_{12} 1,6 isomer), 8.67 and 8.60 d (4H, $J = 8.5$ Hz, pery-H_5 and pery-H_{11} 1,7 isomer; pery-H_6 and pery-H_9 1,6 isomer), 8.34 and 8.26 s (4H, pery-H_2 and pery-H_8 1,7 isomer; pery-H_2 and pery-H_5, 1,6 isomer), 7.85 (m, 8H, aniline-H, 1,6 and 1,7 isomers), 7.46 (overlapping d, 8H, phenoxy-H, 1,6 and 1,7 isomers), 7.09 (d, $J = 8.5$ Hz, 8H, phenoxy-H, 1,6 and 1,7 isomers), 7.04 (td, 8H, $J = 25.5$, 8 Hz aniline-H, 1,6 and 1,7 isomers), 1.35 (s, 36H, $-CH_3$, 1,6 and 1,7 isomers). MALDI LRMS (M+1): calculated 1091.1, found 1091.2.

N,N′-Di(4-ethynylbenzene)-1,6-di(4-tert-butylphenoxy)-3,4:9,10-perylenebis(dicarboximide) and N,N′-Di(4-ethynylbenzene)-1,7-di(4-tert-butylphenoxy)-3,4:9,10-perylenebis(dicarboximide) (***5***). **PDI-1** (0.080 g, 0.073 mmol), and $Pd(PPh_3)_4$ (0.0075 g, 0.0065 mmol) were added to a dry round-bottom flask. Anhydrous THF (20 mL), diethylamine (20 mL), and trimethylsilylacetylene (0.05 mL, 0.36 mmol) were added to give a dark red solution which was degassed with N_2. The solution was heated in an oil bath at 55 °C for 4 days, then cooled to room temperature, filtered through Celite, and evaporated to dryness. The red solid was adsorbed on a short plug of basic alumina and the product eluted with dichloromethane. The resulting red solid (**PDI-2**) was used in the following deprotection reaction without further purification. In a round-bottom flask was combined PDI-2, potassium fluoride (0.061 g, 0.65 mmol), and 18-crown-6 ether (0.168 g, 0.636 mmol) in THF (10 mL) and methanol (1 mL) and the mixture was stirred for 75 min. The resulting red mixture was reduced to a powder under vacuum and chromatographed on silica using chloroform. The product was collected once the solvent was changed to 0.5% methanol in chloroform, yielding a red solid (0.044 g, 35% total yield of a mixture of 1,7- and

(42) Brodard, P.; Matzinger, S.; Vauthey, E.; Mongin, O.; Papamicael, C.; Gossauer, A. *J. Phys. Chem. A* **1999**, *103*, 5858–5870.
(43) Song, Y.; Kohlmeir, E. K.; Meade, T. J. *J. Am. Chem. Soc.* **2008**, *130*, 6662–6663.
(44) Robinson, D. B.; Chidsey, C. E. D. *J. Phys. Chem. B* **2002**, *106*, 10706–10713.
(45) Tidswell, I. M.; Ocko, B. M.; Pershan, P. S.; Wasserman, S. R.; Whitesides, G. M.; Axe, J. D. *Phys. Rev. B* **1990**, *41*, 1111.
(46) Lukas, A. S.; Zhao, Y.; Miller, S. E.; Wasielewski, M. R. *J. Phys. Chem. B* **2002**, *106*, 1299–1306.
(47) Boehm, A.; Arms, H.; Henning, G.; Blaschka, P. Aromatic derivatives of 3,4,9,10-perylenetetracarboxylic acids, dianhydrides, and diimides, their preparation and their use. *DE19547209A1*; BASF A.-G., Germany, **1997**.
(48) Iden, R.; Seybold, G. *Ger. Offen.* **1985**, *DE 3434059*; BASF A.-G., Fed. Rep. Ger.

1,6-isomers). ^{1}H NMR ($CDCl_3$): 9.69 and 9.63 d (4H, J = 8.0 Hz, pery-H_6 and pery-H_{12} 1,7 isomer; pery-H_7 and pery-H_{12} 1,6 isomer), 8.72 and 8.65 d (4H, J = 9.0 Hz, pery-H_5 and pery-H_{11} 1,7 isomer; pery-H_6 and pery-H_9 1,6 isomer), 8.38 and 8.30 s (4H, pery-H_2 and pery-H_8 1,7 isomer; pery-H_2 and pery-H_5, 1,6 isomer), 7.65 (td, J = 13, 12.5 Hz 8H, aniline-H, 1,6 and 1,7 isomers), 7.48 and 7.46 d (J = 2.5 Hz, 8H, phenoxy-H, 1,6 and 1,7 isomers), 7.27 (td, 8H, J = 24, 8.5 Hz aniline-H, 1,6 and 1,7 isomers), 7.11 (d, J = 8.0 Hz, 8H, phenoxy-H, 1,6 and 1,7 isomers), 1.35 (s, 36H, $-CH_3$, 1,6 and 1,7 isomers). ESI-LRMS (M+1): calculated 887.3, found 887.5. ESI-HRMS (M+1): calculated 887.3116, found 887.3114. UV−vis ($CHCl_3$): λ_{max} = 551 nm, 518 nm. IR (NaCl): 2360, 2341 (CC), 1701, 1668 (C═O).

Azido-SAM Formation on ITO and Glass. Prior to use, glass slides were washed with acetone, DCM, ethanol, and last DI water and then cleaned in a piranha solution for at least 30 min (piranha = 3:1 v/v sulfuric acid to 30% hydrogen peroxide, CAUTION! Reacts violently with organics!). ITO coated glass slides were not subject to a piranha clean, but were sonicated in a dilute aqueous solution of Alconox for 10 min, washed with solvents (last water), and placed in concentrated sulfuric acid for at least 30 min to generate a dense population of surface hydroxides. Both ITO and glass slides were then rinsed with copious amounts of DI water, dried under a stream of nitrogen, and placed in a Schlenk flask at a pressure of 10^{-4} Torr to remove residual water. The slides were then submerged in a solution of approximately 1 mM 11-azidoundecyltrimethoxysilane in anhydrous toluene. The reaction vessel was then heated at 65−75 °C overnight. After cooling to room temperature, the slides were removed and sonicated in toluene for 5 min after which they were washed with acetone, DCM, ethanol, and water, then dried in a stream of nitrogen. Slides were then placed in an oven at 75 °C for 2−3 days.

Multilayer Fabrication. *Ethynyl-Porphyrin Layers:* A solution of DMSO, containing < 2% water, consisting of 1.3 mM **1**, 0.325 mM $CuSO_4$, 0.358 mM TBTA, and 1.3 mM sodium ascorbate was placed in contact with one side of a SAM functionalized slide. After 10 min, the slide was washed with acetone, dichloromethane, ethanol, and water. *Ethynyl-Perylenediimide Layers*: A 1.3 mM solution of **5** in DMF and NMP was used as described above with 2,5-di-*tert*-butylhydroquinone used in place of sodium ascorbate as the in situ reductant. *Azido-Linker Layers*: A DMSO solution, containing <8% water, was used as described above consisting of 2.2 mM of the selected azide functionalized linker molecule (**2** or **3**), 4.4 mM $CuSO_4$, 4.8 mM TBTA, and 8.9 mM sodium ascorbate.

Results and Discussion

Multilayer Growth. The CuAAC-based LbL assembly technique described in this report uses two self-limiting reactions to add sequential molecular monolayers to a substrate surface (Scheme 1). Instead of employing proctection/deprotection methods to regenerate alkyne or azide functionalities, we have chosen to use symmetric molecules with multiple ethynyl and azido groups. The complete CuAAC reaction of an azido terminated monolayer with a multiethynyl molecule will yield an ethynyl terminated surface. The reaction is repeated using a multiazido linker molecule to regenerate the azide surface.

UV−vis spectroscopy was employed to monitor the assembly of multilayer films grown on transparent oxide surfaces using the CuAAC-based LbL fabrication method. Figure 1 shows absorption spectra taken at each bilayer during the growth of a multilayer on ITO using the multiethynyl functionalized porphyrin **1** and the azido linker **2** through 10 bilayers (one bilayer consists of one ethynyl-porphyrin layer and one azido-linker layer). The multilayer functionalized ITO slide shows a linear increase in absorbance in the Soret region (440 nm, 43 milli-absorbance units

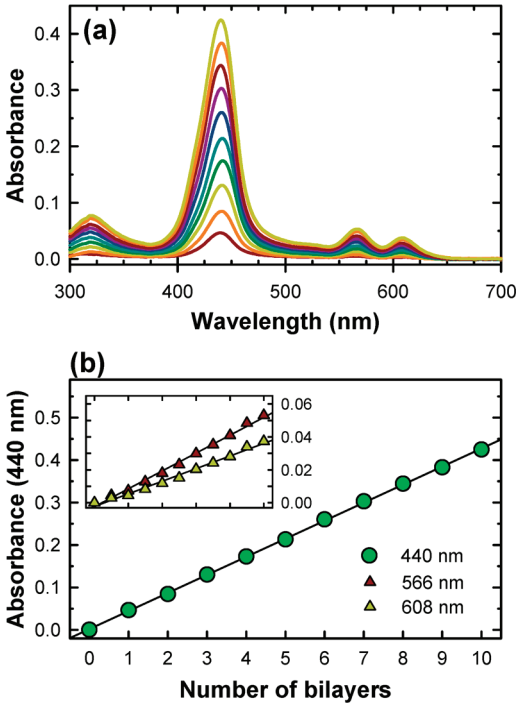

Figure 1. (a) UV−vis absorbance spectra of 1−10 bilayers of **1** and **2** on ITO. (b) Absorbance values at 440 nm for the Soret (circles), and 566 and 608 nm for *Q*-bands (inset, triangles) of **1** vs number of bilayers.

(mAU) per bilayer) and in the *Q*-bands (566 nm, 5.4 mAU/bilayer, 608 nm, 3.8 mAU/bilayer). Molecules **1** and **2** were chosen for the initial LbL growth due to their ability to "regenerate" functional ethynyl and azide groups on the film surface at each step. If the CuAAC reaction failed to generate a full monolayer, the dendritic effect of the molecular components would ensure a high surface density of functional groups for the following reaction step. We believe this approach assists in achieving a high degree of linearity of absorbance increases during multilayer film growth. Notwithstanding, multilayer thin films assembled using **1** and a bis-azido linker, **3**, still show linear growth trends to over 20 bilayers (data not shown).

The extent of monolayer functionalization and rate of multilayer growth can vary from slide to slide depending on the quality of the underlying SAM, the degree of ethynyl-porphyrin functionalization in the initial step, the CuAAC catalyst concentration, and the reaction solvent. The most successful catalyst/solvent combinations, as described in the Experimental Section, were determined from kinetic measurements at various points during the multilayer formation as determined by UV−visible absorption. The catalyst and solvent combinations used throughout this work generally resulted in complete monolayer functionalization in approximately 10−15 min. The quick reactions achieved with the relatively high CuAAC catalyst and substrate concentrations resulted in monolayer films with the highest absorptivities. When lower CuAAC catalyst and/or ethynyl-substrate concentrations were used, the peak absorptivity of the film was lower and subsequent LbL film growth was hindered. We attribute this decrease to incomplete monolayer formation at lower concentrations of **1** possibly due to capping of the azido-SAM with porphyrins attached in a face-on configuration. At higher concentrations of **1**, we surmise that the nearly vertical, densely packed alignment of porphyrins is favored, yielding a surface fully terminated in ethynyl groups. This mechanism is supported by

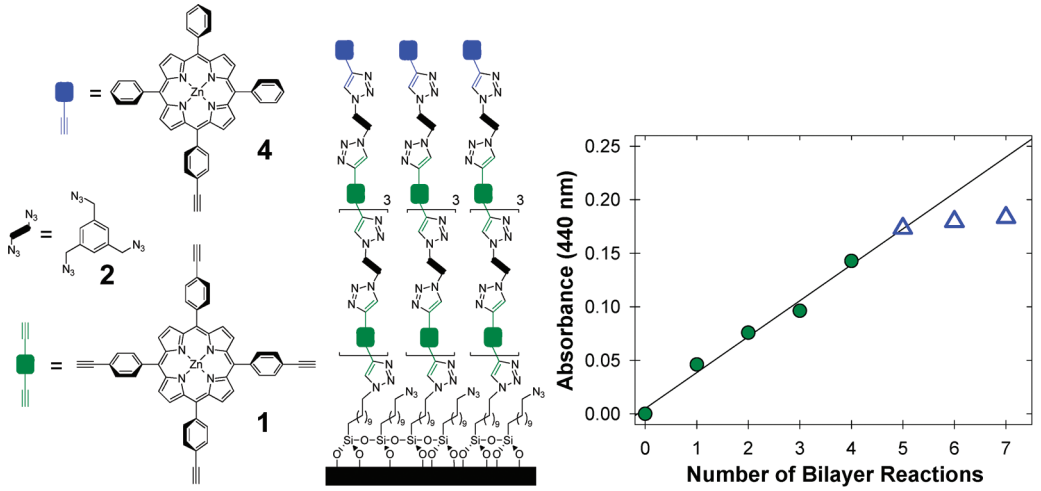

Figure 2. Absorbance values at 440 nm (Soret peak for **1** and **4**) vs number of bilayer reactions. The first four bilayer reactions use **1** and **2**, enabling continued multilayer growth (green circles). Starting with the fifth bilayer reactions, **4** is substituted for **1**, yielding a capping layer that is no longer capable of supporting multilayer growth (blue triangles). Further reactions do not yield appreciable absorptivity increases in the Soret region.

control experiments using a substrate molecule with only one pendant ethynyl group, restricting it to single point attachment to the SAM surface. The maximum absorption achieved for a monolayer of **4** closely matched the absorptivity found for a monolayer of **1** formed under optimized conditions.

As further evidence to show that the increase in absorbance is, in fact, due to multilayer growth via CuAAC reactions, a capping experiment was performed using monoethynyl functionalized porphyrin **4**. Four bilayers of **1** and **2** were grown on a glass slide as described above (Figure 2, green circles). Then, a capping monolayer of monoethynyl porphyrin, **4**, was reacted with the surface azides resulting in a layer that could no longer support multilayer growth. As would be expected, further reactions with **2** and **4** did not show a significant increase in the absorbance (Figure 3). The slight increase in absorbance seen for the sixth and seventh steps using **4** is most likely due to reactions with unreacted azides and ethynyl groups *within* the multilayer and not at the surface. The rate of growth is negligible when compared to the growth for the first **5** bilayers. Additionally, multilayer growth is not observed when the copper catalyst is removed from the reaction mixtures.

In an effort to examine the flexibility of the CuAAC-based LbL assembly procedure, we chose to build multilayers using bis-ethynyl functionalized perylene diimide **5**. Figure 3 shows the absorption spectra taken during the perylene diimide multilayer film assembly through four bilayers. Again, the spectra show a linear increase in absorption intensity for the perylene diimides with each bilayer added. The rate of increase in absorbance at 510 nm (9.5 mAU/bilayer) is much less than the Soret region of the porphyrin multilayer due to the relative differences in molar absorptivity. Though surface orientation and packing density of the films may affect the photophysics of the molecular componenets, the molar absorptivity of perylene diimides are roughly 1/10th that of **1** causing the rate of absorbance growth for perylene diimide multilayers to be significantly less than that of porphyrin multilayers.

So far, we have shown that CuAAC-based LbL construction of multilayer films works well when using a single-component ethynyl-functionalized molecule, but there are several applications where multicomponent assemblies would be beneficial. As a further example of the flexibility of the CuAAC based LbL molecular thin film assembly, we created a mixed multilayer

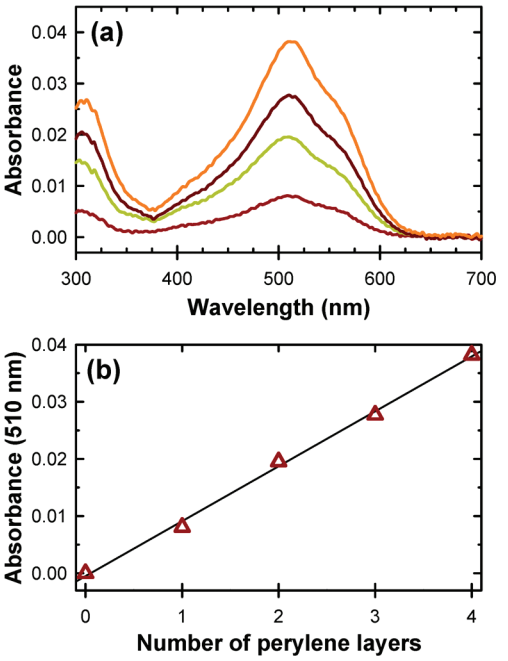

Figure 3. (a) Absorbance profile of bilayers of **5** and **2** on glass. (b) Absorbance value at 510 nm vs number of bilayers.

comprising alternating bilayers of porphyrin **1** and perylene diimide **5**, with **2** as the multiazido linker. The multilayer is grown in an alternating fashion incorporating both porphyrin and perylene diimide molecules with a linker molecule between each dye layer. Figure 4b shows the UV−vis spectra for 1 through 8 molecular bilayers (four bilayers of **1** and **2** and four bilayers of **5** and **2**). Green and red trends represent the spectra taken after the addition of a layer of **1** and **5**, respectively. The first molecule reacted with the SAM functionalized slide is **1**, resulting in a large increase in Soret absorbance at 440 nm, and a slight increase for *Q*-bands (above 550 nm). After the addition of a layer of **2**, a monolayer of **5** is added to the film. This action does not significantly affect the absorbance at 440 nm but does result in an increase at 518 nm. Upon addition of another layer of **1**, the absorbance at 440 nm increases significantly while the absorbance at 518 does not. This alternating pattern continues with an

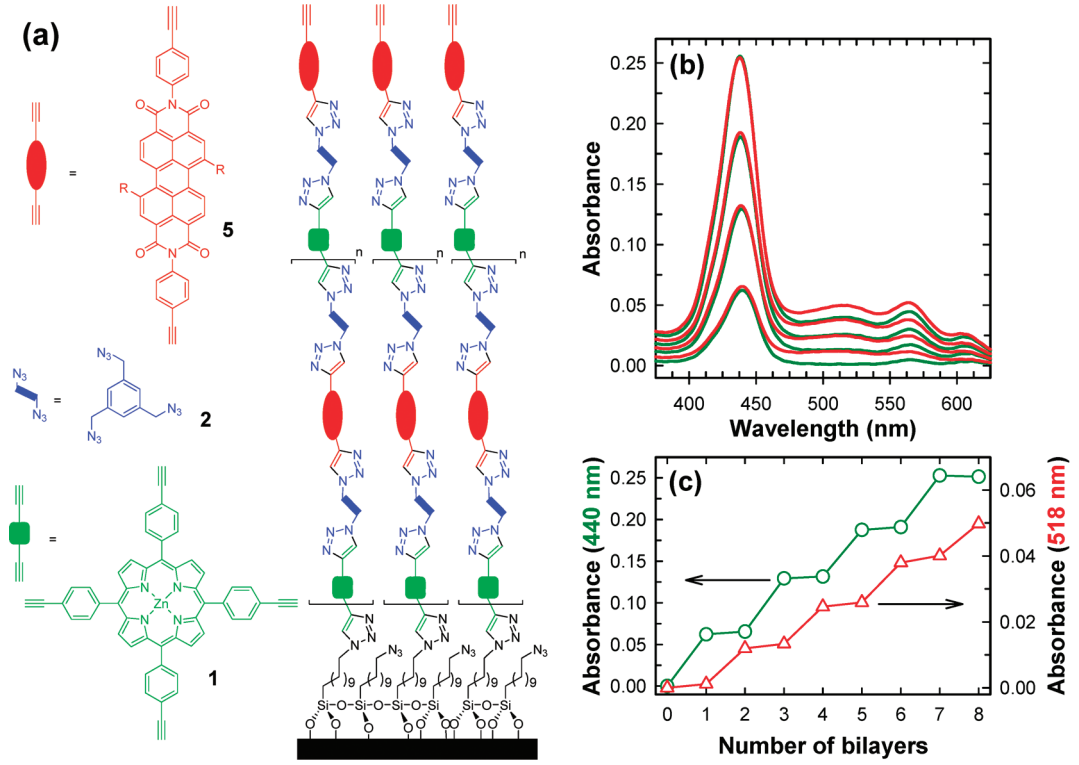

Figure 4. (a) Idealized mixed multilayer containing **1** and **5** grown in an alternating fashion with azido linker **2**. (b) Absorbance profiles of a mixed multilayer (8 bilayers). Green lines represent spectra taken after the addition of a layer of **1** and red lines after the addition of a layer of **5**. (c) Absorbance at 440 nm (green circles) and 515 nm (red triangles) vs number of bilayers.

increase in absorbance at 440 nm with bilayers of **1** and **2** and increases at 518 nm with bilayers of **5** and **2** (Figure 4c). The rate of increase at 440 nm (porphyrin Soret) is again much greater than the rate of increase at 518 nm (perylene diimide max) due to the relative differences in molar absorptivity. The fabrication of a mixed multilayer using alternating porphyrin and perylene diimide molecular components highlights the versatility of using CuAAC as a coupling method for molecular LbL thin film assembly.

Multilayer Optical Properties. The absorbance profile of a multilayer of **1** on a glass surface shows a bathochromic shift and broadening compared to the solution spectrum (Supporting Information Figure S1, 422 nm Soret in DCM vs 440 nm for surface bound multilayer). These spectral changes suggest the porphyrin layers are forming J-type aggregates within the thin-film structure as predicted by exciton theory.[49] Porphyrin aggregation is a common occurrence within LbL assembled thin films and is the result of strong intermolecular $\pi-\pi$ interaction of the planar molecules, resulting in similar spectral shifts to those observed in multilayers of **1** and **2**.[50−54] The absorbance profiles of multilayers of **5** also display aggregation induced spectral deviations from solution absorbance profiles (Supporting Information Figure S2). As with the porphyrin based multilayers, the absorbance profile of the perylene diimide is significantly broadened as compared to the solution spectra. Unlike the porphyrin, the perylene diimide multilayers do not display a bathochromic shift in the absorption bands. Rather, the absorption bands appear at roughly the same wavelength, but the intensity of the higher energy band at 510 nm is enhanced over that of the lower energy band at 552 nm. This reversal of absorption band intensity is often observed for dimers or H-type aggregates of perylene diimides.[55,56] A vibronic treatment of the molecular excitonic coupling theory predicts that the $v = 0$ vibronic level transition becomes symmetrically disallowed, while the $v = 1$ vibronic level gains in intensity.[55−58] Similar spectral features were observed with perylene diimide multilayers grown using zirconium phosphonate interlayer connections.[59,60] The propensity of these porphyrin and perylene diimide materials to aggregate may invoke some self-assembly processes in the formation of the multilayer films and assist in long-range ordering.[10]

Polarized absorption measurements were performed to investigate the presence of structural order within the multilayer films of **1** and **2**.[61−64] Figure 5a shows the absorbance spectra of a multilayer film consisting of five bilayers of **1** and **2** on glass with the slide held at 45° with respect to the incoming light path. The

(49) Bohn, P. W. *Annu. Rev. Phys. Chem.* **1993**, *44*, 37–60.
(50) Abdelrazzaq, F. B.; Kwong, R. C.; Thompson, M. E. *J. Am. Chem. Soc.* **2002**, *124*, 4796–4803.
(51) Splan, K. E.; Hupp, J. T. *Langmuir* **2004**, *20*, 10560–10566.
(52) Qian, D.-J.; Wakayama, T.; Nakamura, C.; Miyake, J. *J. Phys. Chem. B* **2003**, *107*, 3333–3335.
(53) Qian, D.-J.; Nakamura, C.; Miyake, J. *Chem. Commun.* **2001**, 2312–2313.
(54) Qian, D.-J.; Nakamura, C.; Ishida, T.; Wenk, S.-O.; Wakayama, T.; Takeda, S.; Miyake, J. *Langmuir* **2002**, *18*, 10237–10242.
(55) van der Boom, T.; Hayes, R. T.; Zhao, Y.; Bushard, P. J.; Weiss, E. A.; Wasielewski, M. R. *J. Am. Chem. Soc.* **2002**, *124*, 9582–9590.
(56) Wasielewski, M. R. *Acc. Chem. Res.* **2009**, *42*, 1910–1921.
(57) Oddos-Marcel, L.; Madeore, F.; Bock, A.; Neher, D.; Ferencz, A.; Rengel, H.; Wegner, G.; Kryschi, C.; Trommsdorff, H. P. *J. Phys. Chem.* **1996**, *100*, 11850–11856.
(58) Robert, L. F.; Martin, G. *J. Chem. Phys.* **1964**, *41*, 2280–2286.
(59) Cho, K. J.; Shim, H. K.; Kim, Y. I. *Synth. Met.* **2001**, *117*, 153–155.
(60) Martinson, A. B. F.; Massari, A. M.; Lee, S. J.; Gurney, R. W.; Splan, K. E.; Hupp, J. T.; Nguyen, S. T. *J. Electrochem. Soc.* **2006**, *153*, A527–A532.
(61) Massari, A. M.; Gurney, R. W.; Wightman, M. D.; Huang, C. H. K.; Nguyen, S. B. T.; Hupp, J. T. *Polyhedron* **2003**, *22*, 3065–3072.
(62) Aramata, K.; Kamachi, M.; Takahashi, M.; Yamagishi, A. *Langmuir* **1997**, *13*, 5161–5167.
(63) Azumi, R.; Matsumoto, M.; Kawabata, Y.; Kuroda, S.; Sugi, M.; King, L. G.; Crossley, M. J. *J. Phys. Chem.* **1993**, *97*, 12862–12869.
(64) Yoneyama, M.; Sugi, M.; Saito, M.; Ikegami, K.; Kuroda, S.; Iizima, S. *Jpn. J. Appl. Phys.* **1986**, *25*, 961–965.

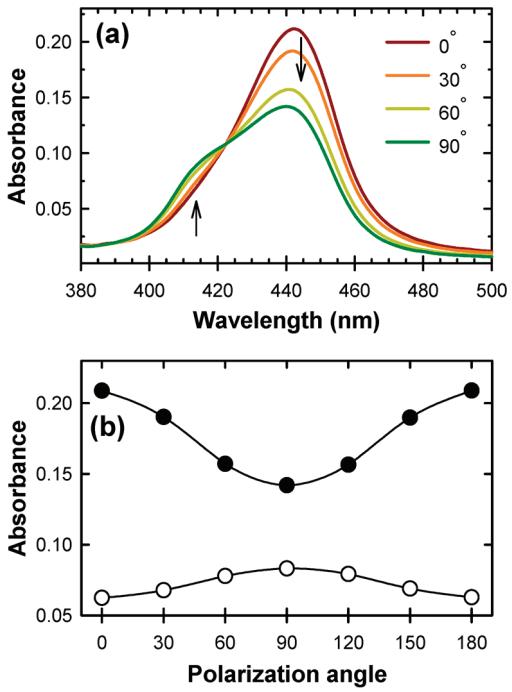

Figure 5. (a) Polarized absorbance profile of five bilayers of **1** and **2** on glass at 0°, 30°, 60°, and 90° polarization angle (120°, 150°, 180° omitted for clarity, but generally overlaid the profiles of 60°, 30°, and 0°, respectively). Arrows indicate direction of absorbance change from 0° to 90°. (b) Absorbance values vs polarization angle at 440 nm (filled circles) and 414 nm (open circles).

angle of the polarization vector of the incoming light was varied from 0° to 180° in 30° increments. The absorbance at the Soret peak (440 nm) reaches a maximum with vertically polarized light (0° and 180°) and a minimum with horizontally polarized light (90°). A similar trend is observed for both of the *Q*-bands at 566 and 608 nm (data not shown). A shoulder on the high energy side of the Soret peak at 412 nm follows an opposite trend, reaching a maximum absorbance at a polarization angle of 90° and a minimum at 0° and 180°. The two polarization trends highlight independent electronic transitions that make up the porphyrin Soret absorbance. The film's polarization dependence implies that the transition dipole moments have a component oriented along a vector normal to the substrate surface. Thus, this suggests the molecules themselves have an average orientation with the porphyrin ring aligned with respect to the surface normal resulting in the ordering of the thin film materials. The same trend is seen at any point during multilayer growth (data not shown) implying that from the addition of the first monolayer the films remain ordered in the same general fashion. Absorption measurements with the slide positioned normal to incoming light beam show no polarization dependence indicating that the porphyrin molecules are randomly oriented within the plane of the glass substrate.

Water Contact Angle. The surface compositions of the multilayer films were probed using sessile drop water contact angle measurements. It is expected that physical surface properties of the multilayer films will change with the addition of alternating ethynyl and azido layers. Figure 6 shows the contact angles and absorbance for the Soret maximum at 440 nm during the assembly of five bilayers of **1** and **2** on a glass substrate. A very low, almost completely wetting value is observed for the cleaned glass slide (Figure 6, layer −1) which implies a high density of surface hydroxides (very hydrophilic). Following the addition of

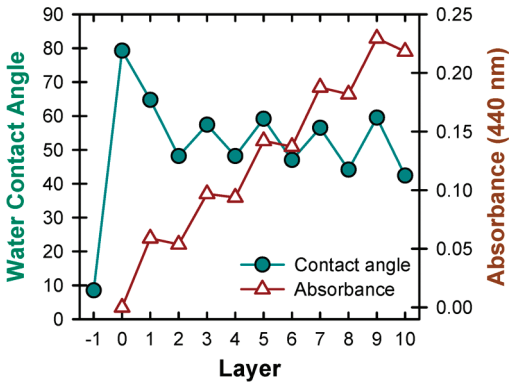

Figure 6. Water contact angles (green filled circles) and absorbance values at 440 nm (red open triangles) for 5 bilayers of **1** and **3** grown on glass. Layer −1 is a freshly cleaned glass slide; layer 0 is the glass slide functionalized with the 11-azidoundecylsiloxane SAM. Error bars were omitted because the circular symbols are larger than the error measurements.

the 11-azidoundecylsiloxane SAM to the glass surface, the water contact angle increases significantly to 80° (Figure 6, layer 0). This value is similar to that observed for an azido-hexydecenylsiloxane SAM formed on glass.[65] Once the azide-functionalized SAM is reacted with **1**, the water contact angle decreases to 64.8° (Figure 6, layer 1). During multilayer formation, a clear trend is observed for layers 1−10 where the azide terminated surfaces consistently produce a lower water contact angle (even numbered layers, average = 46.0°) than the alkyne terminated surfaces (odd numbered layers, average = 59.5°). Similar trends were also observed when using **2** as the azido linker. It is inferred that the polar nature of the azide group, compared to ethynyl, results in a lower water contact for the azide-terminated linker layers. These results provide evidence that surface properties of the multilayer alternate in a well-defined manner suggesting stratification of the molecular building blocks and nearly complete monolayer formation at every layer.

X-ray Reflectivity (XRR). We employed grazing angle X-ray reflectivity (XRR) to examine the height, roughness, and density of multilayers of **1** and **3** grown on glass.[66,67] XRR has been used in the past to examine the thickness and structure of films grown using various LbL techniques.[7,9,10,68] Briefly, grazing angle incident X-ray beams on a surface coated with a thin film generate reflections from both the film and substrate surfaces, resulting in constructive and destructive interference of the light beam. The measured reflectivity at increasing angles show characteristic fringe peaks that depend on the overall film thickness, roughness, and density. Figure 7 shows the XRR data (open circles) and simulations (solid lines) of an 11-azidoundecylsiloxane SAM (black line) and 5 and 10 bilayers of **1** and **3** grown glass (red and green lines, respectively). The XRR data for the 11-azidoundecylsiloxane SAM on glass show only a single minimum, while the samples with 5 and 10 bilayers of **1** and **3** show multiple fringe peaks. As can be expected, the fringe patterns shift to lower angles or wave vector transfer (q) as the film thickness increases from 5 to 10 bilayers. Fitting of the XRR scans resulted in a thickness of 1.5 nm for the 11-azidoundecylsiloxane SAM and 13.1 and 23.1 nm for 5 to 10 bilayers of **1** and **3** on glass, respectively.

(65) Balachander, N.; Sukenik, C. N. *Langmuir* **1990**, *6*, 1621–1627.
(66) Chason, E.; Mayer, T. M. *Crit. Rev. Solid State Mater. Sci.* **1997**, *22*, 1–67.
(67) Holy, V.; Pietsch, U.; Baumbach, T. *High-Resolution X-Ray Scattering from Thin Films and Multilayers*; Springer: Berlin, 1999; Vol. *149*.
(68) Evmenenko, G.; Boom, M. E. v. d.; Kmetko, J.; Dugan, S. W.; Marks, T. J.; Dutta, P. *J. Chem. Phys.* **2001**, *115*, 6722–6727.

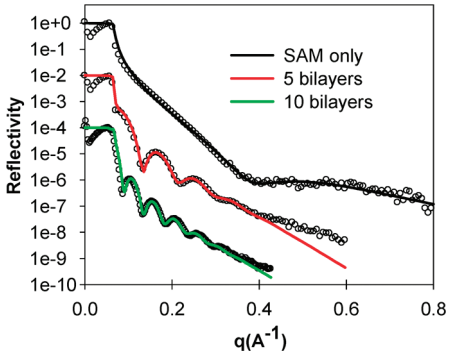

Figure 7. XRR data (open circles) and simulations (solid lines) of an 11-azidoundecylsiloxane SAM (black line) and 5 and 10 bilayers of **1** and **3** grown glass (red and green lines, respectively) vs the wave vector transfer (q). The data for 5- and 10-bilayer samples are offset for clarity.

Thus, multilayers of **1** and **3** grown using the CuAAC LbL assembly technique average 2.5 nm per bilayer. Additionally, the rms roughness values for the films increases slightly with thickness: 1.50 and 1.8 nm for 5 and 10 bilayers of **1** and **3** on glass, respectively. Further detailed studies on the thickness and morphology of thin films assembled using CuAAC reactivity on Si substrates are in being prepared for a subsequent publication.[69]

Electrochemistry. The electrochemical responses of multilayer films grown with the CuAAC-based LbL technique on ITO electrode surfaces are shown in Figure 8. Both of the molecular building blocks used in the fabrication of the multilayer structures are known to exhibit electrochemical activity; meso-tetraphenyl-Zn-porphyrins typically display two single electron oxidation waves at moderate potentials,[70] while phenol substituted perylene diimides undergo two single electron reductions.[71]

Figure 8a (red trace) shows two chemically reversible one electron oxidation waves at $E^{0/+1} = +0.82$ and $E^{+1/+2} = +1.12$ V vs Ag/AgCl for a single monolayer of **1** on an 11-azidoundecylsiloxane SAM formed on ITO at a scan rate, $\upsilon = 1$ V/s. Integration of the cyclic voltammogram (CV) gives an effective surface coverage of $\Gamma_{eff} = 1.25 \times 10^{14}$ molecules/cm^2 (Table 1) or a molecular footprint of 80 Å^2/molecule. The Faradaic waves for the porphyrin are significantly broader ($\Delta E_{p,1/2} \approx 180$ and 145 mV for the first and second oxidation waves, respectively) than expected for an ideal Nernstian reaction of a surface bound species ($\Delta E_{p,1/2} = 90.6$ mV) due to Coulombic interaction between molecules within the densely packed monolayer.[72−74] The anodic and cathodic waves are split significantly which increases with faster voltammetric scan rates due to rate limiting electron transfer through the SAM.[32] Additionally, modest resistance in the ITO electrode imparts some offset in the voltammetric scans, adding to the apparent peak splitting. As expected, the charge increases with the addition of more porphyrin layers to the multilayer structure. The resulting CVs display increased peak broadening and splitting as additional layers are added to the ITO surface.

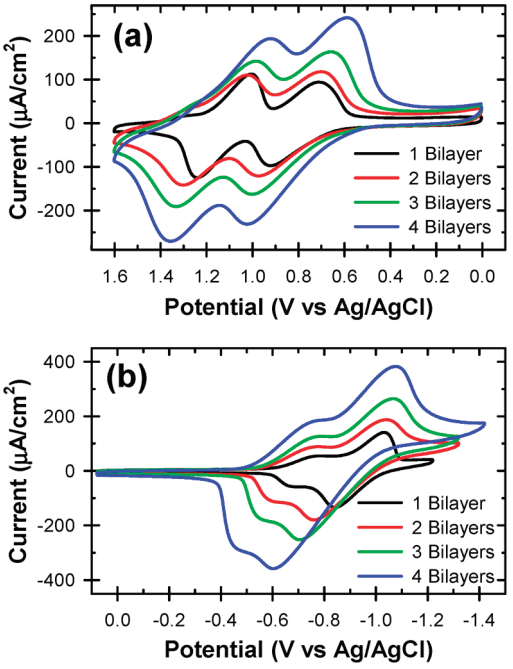

Figure 8. (a) Cyclic voltammetric current response vs potential for 1−4 bilayers of **1** and **2** on ITO. (b) Cyclic voltammetric current response vs potential for1−4 bilayers of **5** and **2** on ITO. All scans were taken at a scan rate of 1 V/s with the ITO set as the working electrode in contact with 0.1 M TBAP in anhydrous DCM under an N_2 atmosphere.

Figure 8b shows similar electrochemical results for 1−4 bilayers of **5** and **2** on ITO. **5** displays two chemically reversible single electron reductions in DCM at $E^{0/-1} = -0.64$ and $E^{-1/-2} = -0.81$ V vs Ag/AgCl (Supporting Information Figure S5). A monolayer of **5** on an 11-azidoundecylsiloxane SAM formed on ITO at a scan rate, $\upsilon = 1$ V/s displays two quasi reversible waves at $E^{0/-1} = -0.73$ and $E^{-1/-2} = -0.94$ V vs Ag/AgCl. The first reduction wave contains approximately one-third of the charge of the second. The asymmetry of the two reduction waves could be the result of the high packing density and aggregation of the perylene diimide monolayer. Similar asymmetric CVs were observed for metal bisphosphonate multilayers of perylene diimides on ITO.[59] Integration of the CV for the monolayer in Figure 8b, assuming a 2 e$^-$ reduction of each perylene diimide, gives an effective surface coverage of $\Gamma_{eff} = 1.0 \times 10^{14}$ molecules/cm^2 (Table 1) or a molecular footprint of 99 Å^2/molecule. Similar to the porphyrin, multilayers grown with **5** and **2** show an increase in the charge passed, a broadening in peak shape and increased peak splitting with each additional bilayer added to the ITO electrode surface. Attempts to examine the electrochemical properties of a mixed multilayers of **1** and **5** were hindered by irreversible oxidation of **5** at a potential similar to oxidation of **1** (Supporting Information Figure S4).

Table 1 shows the calculated charge density and effective molecular coverages determined through integration of the CV for multilayer of both **1** and **5**. The total charge density of the films increases systematically with each additional layer added to the ITO electrode. The increase in charge density is highest for the first layer but roughly follows a linear trend and mirrors the absorbance profile changes (Supporting Information Figure S5). Examination of the CV's in Figure 8 reveal the lack of any Faradaic waves in the potential range where Cu-TBTA and/or $CuSO_4$ would appear, suggesting that significant amounts of Cu

(69) Palomaki, P. K. B.; Krawicz, A.; Dinolfo, P. H., to be submitted.
(70) Wahab, A.; Bhattacharya, M.; Ghosh, S.; Samuelson, A. G.; Das, P. K. *J. Phys. Chem. B* **2008**, *112*, 2842–2847.
(71) Zhao, C.; Zhang, Y.; Li, R.; Li, X.; Jiang, J. *J. Org. Chem.* **2007**, *72*, 2402–2410.
(72) Bard, A. J.; Faulkner, L. R. In *Electrochemical Methods: Fundamentals and Applications*, 2nd ed.; John Wiley & Sons, Inc.: New York, 2001.
(73) Calvente, J. J.; Andreu, R.; Molero, M.; Lopez-Perez, G.; Dominguez, M. *J. Phys. Chem. B* **2001**, *105*, 9557–9568.
(74) Chidsey, C. E. D.; Bertozzi, C. R.; Putvinski, T. M.; Mujsce, A. M. *J. Am. Chem. Soc.* **2002**, *112*, 4301–4306.

Table 1. Electrochemical Data: Charge Density (σ) and Effective Surface Coverage (Γ_{eff}) of the Multilayer Thin Films

multilayer components	number of bilayers	σ (μC cm^{-2})	Γ_{eff} (molecules cm^{-2})
1 and **2**	1	40	1.3×10^{14}
	2	58	1.8×10^{14}
	3	79	2.5×10^{14}
	4	121	3.8×10^{14}
	5	148	4.6×10^{14}
5 and **2**	1	32	1.0×10^{14}
	2	67	2.1×10^{14}
	3	95	3.0×10^{14}
	4	149	4.7×10^{14}

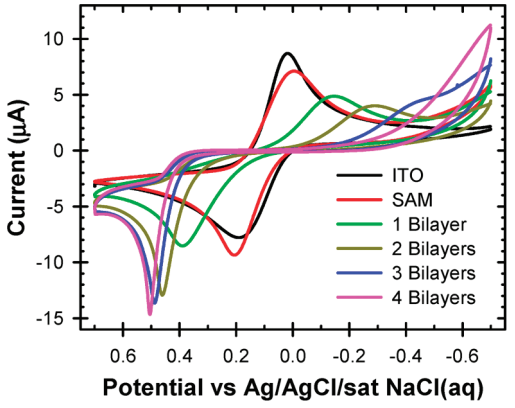

Figure 9. Cyclic voltammetric current response vs potential for a modified ITO electrode in contact with an aqueous solution containing $[Co(bpy)_3]Br_2$ and 0.1 M KCl. The current response from the oxidation and reduction of $[Co(bpy)_3]Br_2$ is shown for freshly cleaned ITO (black), 11-azidoundecylsiloxane SAM modified ITO (red), and 1 (green), 2 (brown), 3 (blue), and 4 (pink) bilayers of **1** and **2** on ITO. CVs were taken at a scan rate, υ = 25 mV/s.

catalysts do not remain in the film.[33,35,75] Analysis of the signal-to-noise ratio of our electrochemical scans leads to an upper limit of electrochemically active Cu species in our films at about 0.1 and 0.25 mol % relative to the perylene and porphyrin molecular building blocks, respectively.

To probe the quality and packing density of the multilayers films, a blocking layer study was performed using $[Co(bpy)_3]^{2+}$ as an electrochemical probe.[76] A chemically reversible one electron wave is observed for the $[Co(bpy)_3]^{2+/3+}$ redox transition using a freshly cleaned (Figure 9, black trace) and an 11-azidoundecylsiloxane modified ITO electrode (Figure 9, red trace). The lack of substantial peak splitting and broadening for the SAM-modified electrode suggests that the 11-azidoundecylsiloxane does not form as dense of a monolayer as alkanethiols on Au(111).[77,78] Upon addition of a monolayer of **1** via the CuAAC reaction, the peak splitting increases drastically to 530 mV (Figure 8, green trace). The increase in overpotential is due to the dense porphyrin monolayer acting as an insulating blocking layer, requiring electrons to tunnel through the film to reach the underlying ITO electrode. Upon addition of a second porphyrin bilayer, the peak splitting increases to 750 mV, and the oxidative peak sharpens drastically. This trend continues for the oxidative peaks for bilayers 2, 3, and 4. We attribute the sharpening oxidative peak to the catalytic oxidation of $[Co(bpy)_3]^{2+}$ by the porphyrin-based multilayer films. The onset of the first porphyrin oxidation for the multilayer film in Figure 8a comes at approximately the same potential as the peaks for $[Co(bpy)_3]^{2+}$ oxidation by films with 2, 3, and 4 bilayers of **1** and **2**. Conversely, the reductive waves show a continued broadening and shifting to more negative values as the insulating layer becomes thicker. The substantial increases in peak splitting for the $[Co(bpy)_3]^{2+/3+}$ redox waves suggests that the multilayer films generated via the CuAAC based LbL assembly scheme are densely packed and pinhole defect-free over the surface area of the electrochemical experiment (~0.15 cm^2).

Conclusion

We have developed a new LbL thin film fabrication process that utilizes CuAAC reactivity in the coupling of molecular building blocks such as porphyrins and perylene diimides. The multilayer films were created by reacting an oxide substrate coated with an azide-terminated SAM with a multiacetylene molecule via CuAAC. Addition of a layer of polyazide linker regenerates an azide-rich surface. This two-step process can be repeated indefinitely to reach any desired number of molecular bilayers. The resulting thin films are electrochemically active over several layers, are pinhole defect-free as determined by electrochemical blocking experiments, and polarized absorption measurements indicate that the molecular components are ordered along a vector normal to the substrate surface.

Arguably, the greatest feature of this LbL assembly method is the ability to incorporate a variety of molecular structures into multilayer thin films together or as single component films. Additionally, the technique provides a rapid interlayer coupling reaction that does not require expensive catalysts or forcing conditions. While further testing will be necessary to determine the scope of this method, it is reasonable to assume that most molecules containing multiple azide or acetylene groups could participate in multilayer formation using this technique. The process outlined here should enable the modification of any substrate that can be functionalized with an azide-terminated SAM. Work on LbL modification of other substrates is currently underway in our group. Additionally, we are examining other experimental techniques to determine the morphology and thickness of the multilayer structures.

Acknowledgment. We would like to thank Prof. Chang Ryu for the use of his group's goniometer and Prof. James Moore for his helpful discussions regarding this manuscript. This work was supported by Rensselaer Polytechnic Institute through faculty start-up funds. P.K.B.P acknowledges a Wiseman Family Fellowship from Rensselaer Polytechnic Institute.

Supporting Information Available: Solution and multilayer absorption profiles of **1** and **5**, solution electrochemistry of **5**, cyclic voltammograms of mixed multilayers of **1** and **5**, and plots comparing multilayer charge density and absorptivity. This material is available free of charge via the Internet at http://pubs.acs.org.

(75) Donnelly, P. S.; Zanatta, S. D.; Zammit, S. C.; White, J. M.; Williams, S. J. *Chem. Commun.* **2008**, 2459–2461.
(76) Hillebrandt, H.; Tanaka, M. *J. Phys. Chem. B* **2001**, *105*, 4270–4276.
(77) Chidsey, C. E. D.; Loiacono, D. N. *Langmuir* **1990**, *6*, 682–691.
(78) Porter, M. D.; Bright, T. B.; Allara, D. L.; Chidsey, C. E. D. *J. Am. Chem. Soc.* **1987**, *109*, 3559–3568.